International Journal of Applied Power Engineering (IJAPE)
Vol. 15, No. 3, September 2026, pp. 1253~1263
ISSN: 2252-8792, DOI: 10.11591/ijape.v15.i3.pp1253-1263

Advanced wireless electric vehicle charging system with cascaded fuzzy control and multi-stage rectification

Naveena Sandhadi, Srinu Naik Ramavathu
Department of Electrical Engineering, Andhra University, Visakhapatnam, India

Article Info

Article history:

Received Oct 16, 2025
Revised Apr 2, 2026
Accepted Jun 9, 2026

Keywords:

Cascaded fuzzy controller
Electric vehicles
Isolation transformer
Proportional-integral
Three-stage synchronous rectifier
Vienna rectifier

ABSTRACT

The growing demand for electric vehicles (EVs) has intensified the need for high-efficiency, reliable, and user-friendly wireless charging systems. Conventional wired chargers and existing wireless solutions often suffer from high losses, poor power quality, and limited control accuracy under dynamic operating conditions. To address these challenges, this paper proposes an advanced wireless charging architecture integrating a three-phase Vienna rectifier, high-frequency inverter, and isolation transformer. A three-phase frequency inverter and a three-stage synchronous rectifier further enhance conversion efficiency. Precise voltage and current regulation is achieved using a cascaded fuzzy controller (CFC) combined with a proportional–integral (PI) controller. MATLAB simulations demonstrate unity power factor, improved efficiency, and stable performance under varying load conditions. The results confirm that the proposed architecture offers a scalable, robust, and energy-efficient solution capable of advancing EV charging infrastructure and supporting sustainable transportation.

Corresponding Author:

Naveena Sandhadi
Department of Electrical Engineering, Andhra University
Visakhapatnam, India
Email: sandhadinaveena211@gmail.com

1. INTRODUCTION

Electric vehicles (EVs) represent a pivotal shift toward sustainable transportation, driven by the urgent need to reduce dependence on fossil fuels and minimize greenhouse gas emissions [1], [2]. As EV adoption increases globally, the demand for efficient, reliable, and user-friendly charging infrastructure has grown considerably. Traditional wired charging systems, though widely used, often fail to meet evolving expectations in terms of operational convenience, efficiency, and long-term durability [3]. These constraints have encouraged the exploration of emerging technologies that can better support the next generation of EV users [4]. Among these, wireless power transfer (WPT) has gained significant attention due to its potential to enhance user convenience, eliminate physical connectors, and reduce mechanical wear in charging systems [5], [6].

Despite its advantages, wireless charging introduces several technical challenges, such as optimizing energy-transfer efficiency, mitigating electromagnetic interference, ensuring safety, and maintaining thermal stability during high-power operation [7]–[9]. The growing complexity of EV power electronic interfaces further increases the need for advanced conversion systems capable of handling high efficiency and fast-charging requirements. Typically, an EV charger consists of two functional stages: one that delivers power from the AC grid to the DC link, and another that transfers energy from the DC link to the battery [10], [11]. In this context, the AC-DC conversion stage is critical, and both the bidirectional inverter and the unidirectional Vienna rectifier are widely considered for this purpose due to their power-handling capabilities and efficiency characteristics [12]. The Vienna rectifier, in particular, is preferred for high-efficiency applications because of its simple structure and suitability as a PWM converter for grid-side current control [13].

However, traditional Vienna rectifiers face control challenges. Their effective operation requires the voltage and current to maintain the same sign—a condition essential for reducing harmonic distortion and ensuring proper current shaping [14]. Violating this requirement results in degraded current quality and increased total harmonic distortion (THD) [15]. Conventional PI controllers, which regulate mainly DC components, often respond too slowly to control alternating currents accurately, leading to increased THD in line currents, especially under high-frequency or low-power conditions [16]–[20]. Alternatives such as PID controllers offer improved accuracy through proportional, integral, and derivative action but suffer from tuning difficulty, sensitivity to noise, and reduced robustness. Similarly, sliding mode controllers (SMC) provide strong robustness and fast dynamics but introduce chattering, resulting in switching stress, EMI issues, and efficiency degradation [21], [22]. Fuzzy logic controllers (FLC) have been explored due to their ability to handle nonlinearities and uncertainties [23]-[27], yet they depend heavily on expert-defined rule bases, limiting adaptability.

To address these limitations, this paper proposes a novel wireless EV charging architecture supported by an advanced three-stage synchronous rectifier and a cascaded fuzzy controller (CFC). The cascaded configuration improves flexibility in tuning, reduces sensitivity to parameter variations, and avoids reliance on a single monolithic fuzzy rule base. Furthermore, the proposed charging system incorporates a Vienna rectifier for AC–DC conversion, a three-phase high-frequency inverter for DC–AC conversion to support wireless energy transfer, and an isolation transformer for safety and galvanic separation. The integration of the synchronous rectifier architecture aims to improve overall energy conversion efficiency by minimizing rectification losses.

The distinct novelty of this research lies in the integration of a three-stage synchronous rectifier with a CFC specifically tailored for wireless EV charging applications. Unlike conventional control strategies, the proposed cascaded fuzzy structure separates the control tasks into hierarchical loops, enabling improved dynamic response, reduced THD, and enhanced robustness against system nonlinearities. Moreover, the combined use of a Vienna rectifier, high-frequency inverter, and isolation transformer within a unified wireless charging architecture provides a uniquely optimized pathway for high-efficiency AC–DC–AC conversion. This architectural and control-level synergy differentiates the proposed system from existing WPT-based EV charging solutions.

This paper is organized as follows: Section 2 explains the proposed wireless charging architecture. Section 3 presents the modelling of the system components and controllers. Section 4 provides simulation results and analysis, and Section 5 concludes the work. Future work includes developing a hardware prototype to validate the simulation results, implementing bidirectional power flow for V2G applications, and exploring AI-based optimization techniques to further improve system performance under practical operating conditions.

2. PROPOSED SYSTEM DESCRIPTION

The interrelationships among the main components of the proposed system are depicted in Figure 1, where the wireless charging architecture functions as an integrated multi-stage energy-conversion chain. The Vienna rectifier first converts the grid AC supply into a regulated DC link, which serves as the input to the high-frequency inverter. This inverter generates an AC waveform suitable for wireless power transfer through the isolation transformer, which provides galvanic isolation and conditions the transferred energy. The three-stage synchronous rectifier then reconstructs a stable DC output for efficient battery charging. The coordinated action of the cascaded fuzzy controller and PI controller ensures precise current and voltage regulation across all stages, enabling reliable operation and enhanced overall system performance. The proposed wireless charging system employs a series–series (SS) compensation topology.

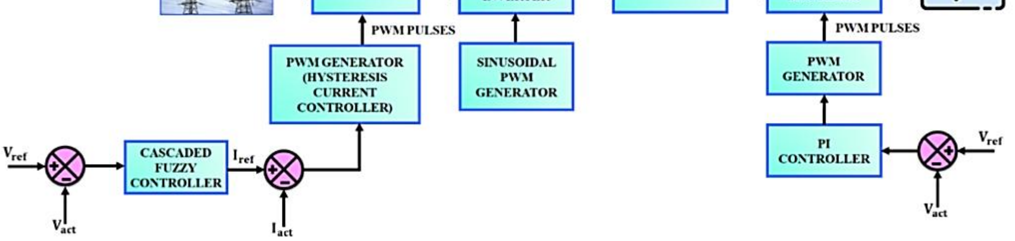

Figure 1. Wireless charging system for EVs using advanced control approach

3. PROPOSED SYSTEM MODELLING

3.1. Modelling of Vienna rectifier

The Vienna rectifier is employed in this work to convert the three-phase grid AC voltage into a regulated DC output. As shown in Figure 2, the topology consists of six diodes and a single active switch configured to maintain balanced current paths. This structure significantly reduces voltage stress on each semiconductor device, as every component is subjected to only half of the total DC bus voltage during operation. As a result, uniformly rated devices can be used across the rectifier, ensuring consistent power dissipation and improved efficiency. To support controller design and system-level coordination, this section provides a detailed mathematical model of the Vienna rectifier. The duty cycle of the active switch is defined based on its switching function, and three distinct operating cases are considered according to the switching state and polarity of the input current.

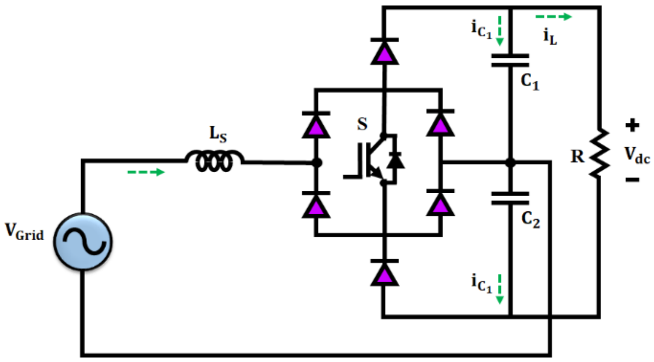

Figure 2. Vienna rectifier circuit

i. Mode 1:

When the active switch is turned on, the inductor current is directed through the switch, and energy is stored in the input inductor. During this interval, the diode paths are blocked, and no capacitor charging occurs. This mode primarily facilitates input current shaping and boost operation.

$$v_s = L_s \frac{di_s}{dt} \tag{1}$$

$$C_1 \frac{dV_{C_1}}{dt} + \frac{V_{C_1}+V_{C_2}}{R} = 0 \tag{2}$$

$$C_2 \frac{dV_{C_2}}{dt} + \frac{V_{C_1}+V_{C_2}}{R} = 0 \tag{3}$$

ii. Mode 2:

When the switch is turned off and the inductor current is positive, the upper diode conducts, allowing the inductor to discharge its stored energy into the upper DC-link capacitor C_1. Consequently, C_1 is charged, and the inductor current decreases while delivering energy to the DC bus.

$$v_s = L_s \frac{di_s}{dt} + V_{C_1} \tag{4}$$

$$i_s = C_1 \frac{dV_{C_1}}{dt} + \frac{V_{C_1}+V_{C_2}}{R} \tag{5}$$

$$C_2 \frac{dV_{C_2}}{dt} + \frac{V_{C_1}+V_{C_2}}{R} = 0 \tag{6}$$

iii. Mode 3:

For a negative inductor current with the switch off, the lower diode path becomes forward-biased, directing current into the lower DC-link capacitor C_2. In this mode, C_2 is charged, and the inductor releases energy symmetrically to the negative half-cycle.

$$v_S = L_s \frac{di_s}{dt} - V_{C_2} \tag{7}$$

$$i_s = -C_2 \frac{dV_{C_2}}{dt} - \frac{V_{C_1}+V_{C_2}}{R} \tag{8}$$

$$C_1 \frac{dV_{C_1}}{dt} + \frac{V_{C_1}+V_{C_2}}{R} = 0 \tag{9}$$

Using the switching function and sign of i_s, the preceding equations are transformed into the following relations to demonstrate the dynamic behaviour of the system.

$$\frac{di_s}{dt} = \frac{1}{L_s}\left[v_s + (s-1)\begin{pmatrix} \frac{1+sign(i_s)}{2} V_{C_1} \\ -\frac{1-sign(i_s)}{2} V_{C_2} \end{pmatrix}\right] \tag{10}$$

$$\frac{dV_{C_1}}{dt} = \frac{1}{C_1}\left[\frac{1+sign(i_s)}{2}(1-S)i_s - \frac{V_{C_1}+V_{C_2}}{R}\right] \tag{11}$$

$$\frac{dV_{C_2}}{dt} = \frac{1}{C_1}\left[\frac{1-sign(i_s)}{2}(1-S)i_s - \frac{V_{C_1}+V_{C_2}}{R}\right] \tag{12}$$

Solving (10)-(12) yields the nonlinear dynamic model of the Vienna rectifier. The selected state variables are structured to facilitate effective control design and ensure accurate representation of system behavior. In this work, the rectifier is regulated using a cascaded FLC, which maintains the DC-link voltage and attenuates input current harmonics. Under this control strategy, the rectifier achieves unity power factor operation, enhancing overall system performance.

3.2. Modelling of cascaded fuzzy logic controller

The output voltage and current of the Vienna rectifier are regulated using a CFC to achieve efficient and stable operation of the wireless EV charging system. Cascade control is particularly advantageous when the primary control loop is affected by strong nonlinearities that limit overall performance. By structuring the controller into two sequential fuzzy loops, disturbances are mitigated and the dynamic response is significantly improved. In this configuration, the outer loop encodes heuristic control knowledge and generates the reference signals, while the inner loop manages nonlinear behavior and executes precise control actions. This dual-loop architecture enhances robustness and ensures superior regulation, as illustrated in Figure 3.

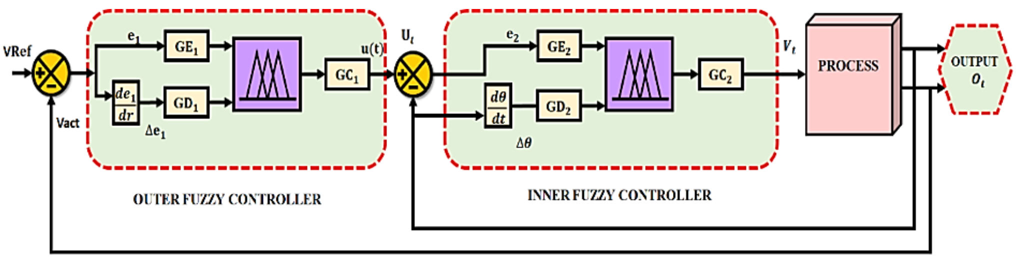

Figure 3. CFC architecture

The following are the regulations used by the fuzzy controller in the outer loop. These regulations are given in (13).

$$R^k : E_i \text{ is } A_1^k \text{ and } \Delta E_i \text{ is } A_2^k \text{ then } U_i = B_K \tag{13}$$

The variables $E_i, \Delta E_i, A_1^k$,and A_2^k are linguistic parameters (fuzzy sets) specified across the appropriate realms of dissertation of change of error and error, U_i is the (control variable) output. B_K is numerical value of management, and R^k indicates the k^{th} rule ($k = 1,2, \dots m$). The standard approach for computing the activation level of every control rule is provided below for both the inner and outer loops.

$$Inner\ loop: w_{1K} = min\{\mu_{A_{1k}(E)}.\mu_{A_{1k}(\Delta E)}\} \tag{14}$$

$$Outer\ loop: w_{2K} = min\{\mu_{A_{1k}(E)}.\mu_{A_{1k}(\Delta E)}\} \tag{15}$$

Each loops' inferred values of control are established as (16) and (17).

$$U_1^* = \frac{\sum_{k=1}^{m} w_{1k} B^k}{\sum_{k=1}^{m} w_{1k}} \tag{16}$$

$$U_2^* = \frac{\sum_{k=1}^{m} w_{2k} B^k}{\sum_{k=1}^{m} w_{2k}} \tag{17}$$

Additionally, certain scaling variables are used to modify the outputs in order to provide the fuzzy controller additional flexibility during optimization.

$$Output\ of\ Outer\ loop: U(t) = U * (t) GC_1 \tag{18}$$

$$Output\ of\ inner\ loop: V(t) = V * (t) GC_2 \tag{19}$$

The membership functions of controller represent the variations and are defined as:

$$NB(-m3), NM(-m2), NS(-m1), ZO(0),$$
$$PS(m1), PM(m2), and\ PB(m3)$$

membership functions of this type have initial values $m1, m2, and\ m3$, respectively.

Figure 4 illustrates the membership function for input E and ΔE. In the inner loop, the fuzzy controller uses the outer loop fuzzy controller as its reference value. Based on outer loop's output, the controller of inner loop regulates the voltage rectifier in system. The system under control has outstanding dynamic features owing to the CFC controller.

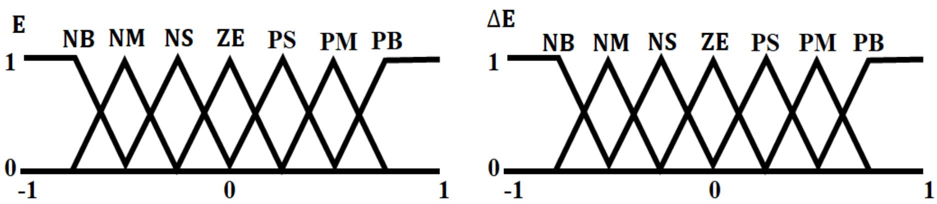

Figure 4. Membership function for input E and ΔE

3.3. Modelling of hysteresis current controller

The hysteresis current controller plays a critical role in regulating the performance of the Vienna rectifier in wireless EV charging applications. It maintains the output current within a predefined hysteresis band, enabling precise tracking of the reference current through direct current regulation. As illustrated in Figure 5, the controller dynamically adjusts the current within this band to determine the appropriate switching state of the rectifier half-bridge. This control approach enhances electromagnetic compatibility (EMC) and minimizes harmonic distortion, which is particularly important in scenarios involving simultaneous charging of multiple EVs. By ensuring stable and bounded current, the hysteresis controller improves overall system performance and enhances the longevity of rectifier components.

3.4. Modelling of isolation transformer

The isolation transformer is a static device designed to provide electrical and physical separation between its primary and secondary windings, ensuring safe energy transfer through magnetic induction. The isolation transformer diagram is shown in Figure 6. It generates an electromotive force (EMF) in the secondary winding while maintaining the same operating frequency as the input. Isolation transformers are employed to step voltage levels up or down, enabling proper matching of voltage and current ratings between interconnected circuits. An essential function of this transformer is the suppression of supply-line voltage spikes, which could otherwise degrade or damage EV batteries. Through galvanic isolation, it enhances system safety, protects sensitive electronic components, and minimizes the risk of electrical shock to users and equipment.

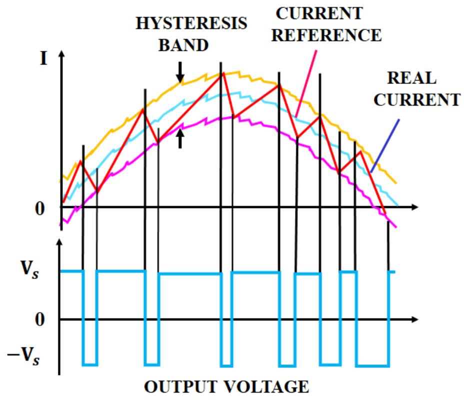

Figure 5. Hysteresis current controller

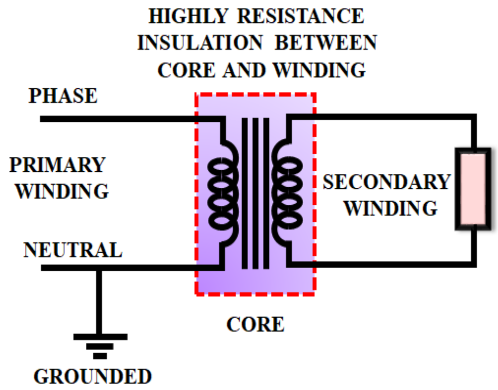

Figure 6. Isolation transformer

3.5. Modelling of three-stage synchronous rectifier

The three-stage synchronous rectifier configuration is illustrated in Figure 7 and consists of a three-stage IGBT inverter bridge, an inductive input interface, and a capacitive DC bus output filter. This topology enhances AC–DC conversion efficiency by improving switching performance and reducing output voltage ripple. Its multi-stage structure also enables better distribution of current stress, thereby increasing reliability during high-power operation. The dynamic behavior of the rectifier is expressed by (20).

$$\vec{v}_s = R.\vec{\imath}_s + L\frac{d\overrightarrow{\imath_s}}{dt} + \vec{v}_{conv} \quad (20)$$

Where $\vec{v}_s$ is the voltage source vector, $\vec{\imath}_s$ is the line current vector and $\vec{v}_{conv}$ is the voltage vector in the terminals of the rectifier.

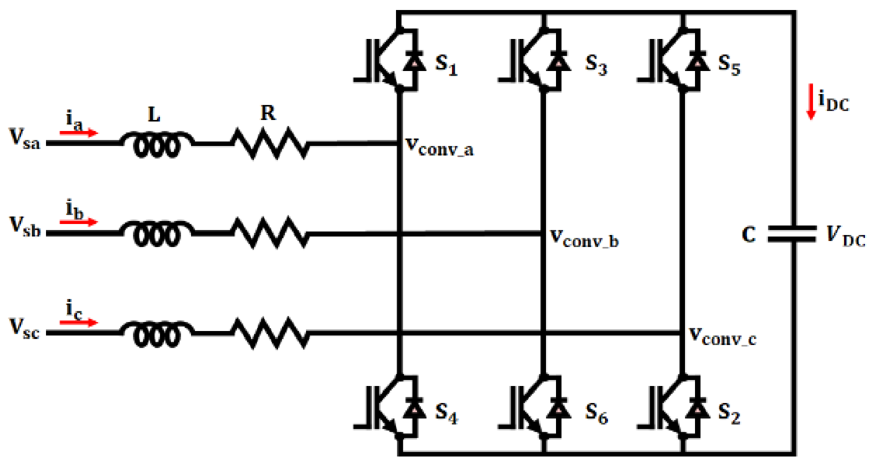

Figure 7. Three-stage synchronous rectifier

4. RESULTS AND DISCUSSION

The performance of the wireless EV charging system with the CFC was evaluated through MATLAB/Simulink simulations. The analysis focuses on power quality, dynamic response, and comparison with existing control approaches to demonstrate the significance of the proposed method. Table 1 presents the key design parameters used for developing the proposed wireless EV charging system, including the specifications of the isolation transformer, switching frequency, and EV battery ratings. These parameters form the foundational configuration for the system's modeling and simulation, ensuring accurate evaluation of charging performance and controller behavior.

The three-phase grid voltage and current waveforms (Figure 8) confirm that the Vienna rectifier maintains a stable sinusoidal input current, indicating effective shaping of the grid current and proper unity power factor operation. The DC-link voltage and power factor response shown in Figure 9 further validate the ability of the CFC to hold the DC-link voltage at its reference while maintaining a power factor close to unity. This demonstrates that the controller minimizes reactive power consumption and ensures efficient energy transfer.

Table 1. Design parameter

Parameter	Specification
Isolation transformer	4.17%
Switching frequency	10 kHz
EV battery	24 Ah, 24 V, 12 Ah,12 V
Rated power for EV Battery	100 Ah

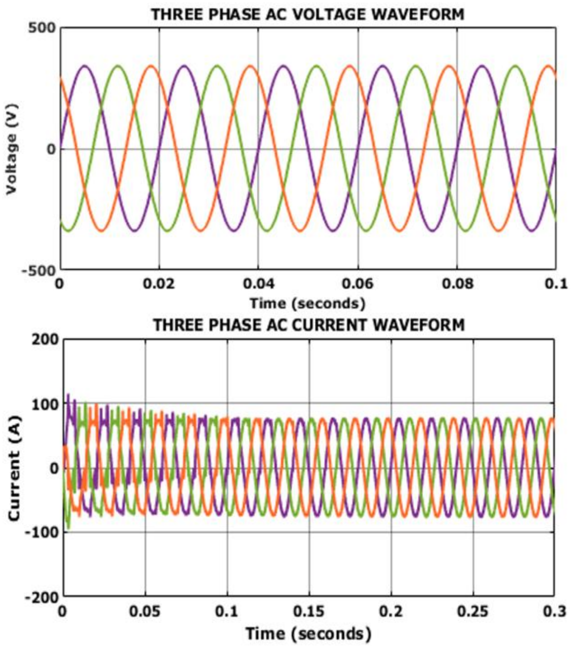

Figure 8. Three phase grid output waveforms of voltage and current

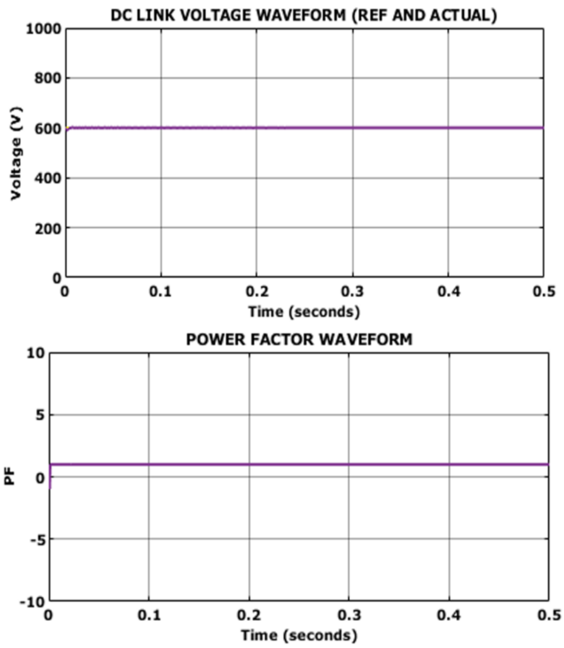

Figure 9. Output waveforms of DC link voltage and power factor

The real and reactive power characteristics illustrated in Figure 10 indicate that the system delivers stable real power while suppressing reactive power almost to zero. This confirms the improvement in power quality compared to conventional controllers. The output voltage of the three-stage synchronous rectifier (Figure 11) remains constant, proving that the multi-stage rectification structure effectively reduces ripple and enhances voltage stability. Figure 12 presents the waveform patterns of both the input AC voltage and the input current over a specific time interval. The voltage and current waveforms are plotted together to illustrate their relationship during the operation of the system under consideration. The high-frequency inverter output (Figure 13) and synchronous rectifier current–voltage characteristics (Figure 14) exhibit stable operation under dynamic loading, showing the system's robustness. These results collectively demonstrate that the proposed architecture ensures consistent power delivery, reduced losses, and improved efficiency across all stages of the charging process.

To evaluate the value and novelty of the proposed controller, comparative performance analyses were performed. Table 2 presents the power factor comparison with established control approaches such as ANFIS, direct power control, and voltage oriented control. The proposed CFC achieves a perfect unity power factor (1.00), outperforming all other methods. Similarly, Table 3 shows that the proposed controller attains the fastest settling time among all evaluated controllers, highlighting its superior dynamic response. The step-response comparison in Figure 15 further confirms this improvement, where the CFC exhibits minimal overshoot and rapid stabilization. This provides clear evidence that the proposed approach is not trivial but significantly advances controller performance for wireless EV charging systems.

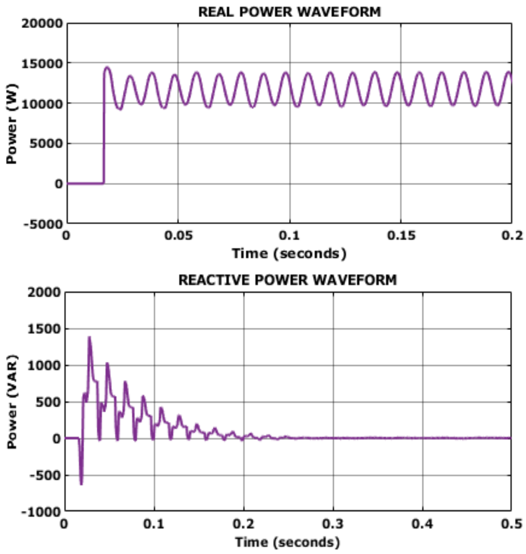

Figure 10. Output waveforms of real and reactive power

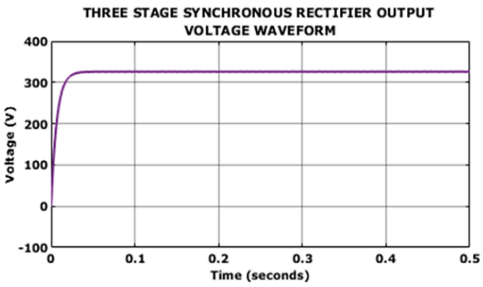

Figure 11. Output voltage waveform of three stage synchronous rectifier

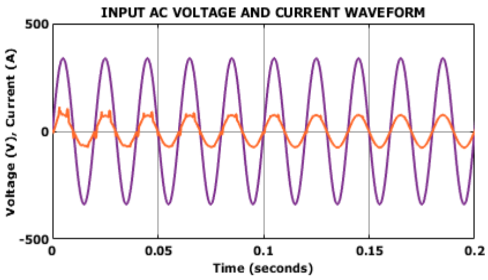

Figure 12. Waveform of input AC voltage and current

Table 2. Performance comparison

Power converter	Controller	Power factor
SEPIC converter	ANFIS controller	89%
Three phase rectifier	Direct power controller	0.92
Vienna rectifier	Voltage oriented controller	96.00%
Proposed Vienna rectifier	CFC controller	1

Table 3. Comparison of settling time

Controller approach	Settling time (s)	Efficiency (%)	THD (%)	EMI suppression
PID controller	0.89	91.8	6.8	Low
Fuzzy controller	0.92	93.2	5.4	Medium
Lyapunov-based optimized FLC	0.96	94.7	4.2	Medium–High
Proposed CFC controller	0.81	97.6	2.9	High

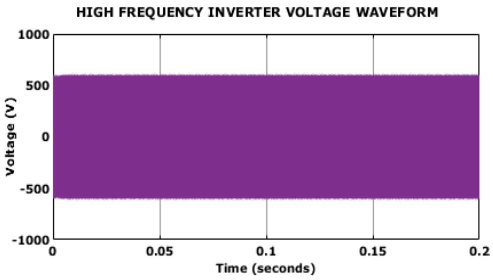

Figure 13. Waveform of high frequency inverter voltage

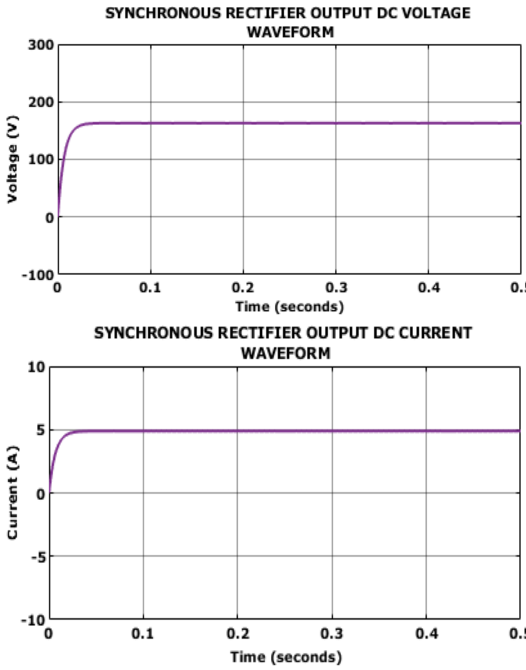

Figure 14. Waveform of synchronous rectifier output DC current and voltage

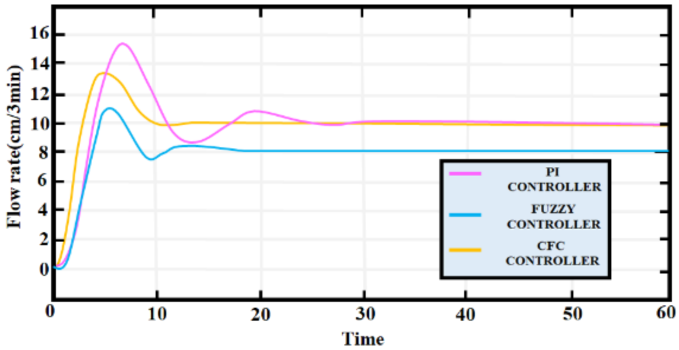

Figure 15. Comparison evaluation of step response

5. CONCLUSION

This paper presents a comprehensive wireless EV charging architecture that integrates a Vienna rectifier, a high-frequency inverter–isolation transformer interface, and a three-stage synchronous rectifier to achieve high-efficiency AC–DC–AC energy conversion. Supported by a CFC and PI controller, the proposed system demonstrates superior voltage and current regulation under dynamic load variations. The simulation results confirm significant quantitative improvements, including unity power factor (1.0), minimized reactive power, stable DC-link voltage regulation, and the fastest settling time of 0.81 s compared to other control strategies. These metrics validate the effectiveness of the multi-stage rectification scheme and the cascaded control approach in enhancing overall charging efficiency and system stability.

The main contributions of this study include: i) the development of a unified multi-stage wireless charging architecture optimized for high-efficiency EV charging, ii) the introduction of a cascaded fuzzy control structure that improves dynamic response and power quality, and iii) the demonstration of enhanced power factor, reduced harmonic distortion, and superior transient behavior relative to existing controllers. Future research will focus on hardware implementation to validate the simulation model, optimization of coil alignment and compensation networks for higher power transfer capability, incorporation of bidirectional power flow for V2G applications, and investigation of AI-based adaptive controllers to further enhance robustness and performance under real-world charging conditions.

FUNDING INFORMATION

The authors declare that no funding was received to support the research work entitled "Advanced wireless electric vehicle charging system with cascaded fuzzy control and multi-stage rectification."

AUTHOR CONTRIBUTIONS STATEMENT

This journal uses the Contributor Roles Taxonomy (CRediT) to recognize individual author contributions, reduce authorship disputes, and facilitate collaboration.

Name of Author	C	M	So	Va	Fo	I	R	D	O	E	Vi	Su	P	Fu
Naveena Sandhadi	✓	✓	✓	✓	✓	✓		✓	✓	✓				
Srinu Naik Ramavathu						✓		✓	✓	✓	✓	✓		

C : **C**onceptualization
M : **M**ethodology
So : **So**ftware
Va : **Va**lidation
Fo : **Fo**rmal analysis
I : **I**nvestigation
R : **R**esources
D : **D**ata Curation
O : Writing - **O**riginal Draft
E : Writing - Review & **E**diting
Vi : **Vi**sualization
Su : **Su**pervision
P : **P**roject administration
Fu : **Fu**nding acquisition

CONFLICT OF INTEREST STATEMENT

The authors state no conflict of interest.

DATA AVAILABILITY

The data that support the findings of this study are available from the corresponding author, [NS], upon reasonable request.

REFERENCES

[1] H. K. Bai *et al.*, "Charging electric vehicle batteries: wired and wireless power transfer: exploring ev charging technologies," *IEEE Power Electronics Magazine*, vol. 9, no. 2, pp. 14–29, 2022, doi: 10.1109/MPEL.2022.3173543.
[2] K. Dimitriadou, N. Rigogiannis, S. Fountoukidis, F. Kotarela, A. Kyritsis, and N. Papanikolaou, "Current trends in electric vehicle charging infrastructure; opportunities and challenges in wireless charging integration," *Energies*, vol. 16, no. 4, 2023, doi: 10.3390/en16042057.
[3] M. Rozman *et al.*, "Smart wireless power transmission system for autonomous EV charging," *IEEE Access*, vol. 7, pp. 112240–112248, 2019, doi: 10.1109/ACCESS.2019.2912931.
[4] A. Ramezani and M. Narimani, "A new wireless EV charging system with integrated DC-DC magnetic element," *IEEE Transactions on Transportation Electrification*, vol. 5, no. 4, pp. 1112–1123, 2019, doi: 10.1109/TTE.2019.2955251.
[5] X. Mou, D. T. Gladwin, R. Zhao, and H. Sun, "Survey on magnetic resonant coupling wireless power transfer technology for electric vehicle charging," *IET Power Electronics*, vol. 12, no. 12, pp. 3005–3020, 2019, doi: 10.1049/iet-pel.2019.0529.
[6] Z. Qian, R. Yan, J. Wu, and X. He, "Full-duplex high-speed simultaneous communication technology for wireless EV charging," *IEEE Transactions on Power Electronics*, vol. 34, no. 10, pp. 9369–9373, 2019, doi: 10.1109/TPEL.2019.2909303.
[7] E. ElGhanam, M. Hassan, A. Osman, and H. Kabalan, "Design and performance analysis of misalignment tolerant charging coils for wireless electric vehicle charging systems," *World Electric Vehicle Journal*, vol. 12, no. 3, p. 89, Jun. 2021, doi: 10.3390/wevj12030089.
[8] M. R. R. Razu *et al.*, "Wireless charging of electric vehicle while driving," *IEEE Access*, vol. 9, pp. 157973–157983, 2021, doi: 10.1109/ACCESS.2021.3130099.
[9] S. Ruddell, U. K. Madawala, and D. J. Thrimawithana, "A wireless EV charging topology with integrated energy storage," *IEEE Transactions on Power Electronics*, vol. 35, no. 9, pp. 8965–8972, 2020, doi: 10.1109/TPEL.2020.2969027.
[10] I. Aretxabaleta, I. M. De Alegria, J. Andreu, I. Kortabarria, and E. Robles, "High-voltage stations for electric vehicle fast-charging: trends, standards, charging modes and comparison of unity power-factor rectifiers," *IEEE Access*, vol. 9, pp. 102177–102194, 2021, doi: 10.1109/ACCESS.2021.3093696.
[11] B. Balasundaram and S. Panchanathan, "Hysteresis current control of Vienna rectifier for electric vehicle charging systems," *Journal of Engineering Science and Technology Review*, vol. 17, no. 2, pp. 182–189, 2024, doi: 10.25103/jestr.172.19.
[12] G. Rajendran, C. A. Vaithilingam, N. Misron, K. Naidu, and M. R. Ahmed, "Voltage oriented controller based Vienna rectifier for electric vehicle charging stations," *IEEE Access*, vol. 9, pp. 50798–50809, 2021, doi: 10.1109/ACCESS.2021.3068653.
[13] S. P. Jose and M. Muthulakshmi, "Vienna rectifier control using SPWM and SVPWM for EV charging station," *Journal of Nuclear Energy Science & Power Generation Technology*, vol. 11, no. 4, pp. 1–6, 2022.
[14] J. Fan, H. Ma, Q. He, L. Fan, and X. Ma, "Modeling and stability analysis of three-phase voltage source Vienna rectifier," *Journal of Electric Power Science and Technology*, vol. 39, no. 1, pp. 243–250, 2024, doi: 10.19781/j.issn.1673-9140.2024.01.025.
[15] D. Molligoda *et al.*, "Hybrid modulation strategy for the Vienna rectifier," *IEEE Transactions on Power Electronics*, vol. 37, no. 2, pp. 1283–1295, 2022, doi: 10.1109/TPEL.2021.3103766.
[16] M. Zhang, Y. Yuan, X. Sun, Y. Zhang, and X. Li, "Harmonic resonance suppression strategy of the front-end Vienna rectifier in EV charging piles," *IEEE Transactions on Power Electronics*, vol. 38, no. 1, pp. 1036–1053, 2023, doi: 10.1109/TPEL.2022.3204537.

[17] A. Ali, J. Chuanwen, Z. Yan, S. Habib, and M. M. Khan, "An efficient soft-switched Vienna rectifier topology for EV battery chargers," *Energy Reports*, vol. 7, pp. 5059–5073, 2021, doi: 10.1016/j.egyr.2021.08.105.

[18] Y. Yuan and Z. Zhang, "A single-phase Vienna rectifier with wide output voltage range," *IEEE Transactions on Transportation Electrification*, vol. 8, no. 3, pp. 3884–3895, 2022, doi: 10.1109/TTE.2022.3153332.

[19] G. Aiello, M. Cacciato, G. Scarcella, G. Scelba, F. Gennaro, and N. Aiello, "Real-time emulation of a three-phase Vienna rectifier with DC voltage control and power factor correction," *Electrical Engineering*, vol. 102, no. 1, pp. 97–106, 2020, doi: 10.1007/s00202-019-00776-y.

[20] X. Yan, F. Qin, J. Jia, Z. Zhang, X. Li, and Y. Sun, "Virtual synchronous motor based-control of Vienna rectifier," *Energy Reports*, vol. 6, pp. 953–963, Dec. 2020, doi: 10.1016/j.egyr.2020.11.098.

[21] N. A. Almamoori, B. Dziadak, and A. H. Sabry, "Design of a closed-loop autotune PID controller for three-phase for power factor corrector with Vienna rectifier," *Bulletin of Electrical Engineering and Informatics*, vol. 11, no. 4, pp. 1798–1806, 2022, doi: 10.11591/eei.v11i4.3728.

[22] H. Ahmed and D. Çelik, "Sliding mode based adaptive linear neuron proportional resonant control of Vienna rectifier for performance improvement of electric vehicle charging system," *Journal of Power Sources*, vol. 542, 2022, doi: 10.1016/j.jpowsour.2022.231788.

[23] H. C. Nannam and A. Banerjee, "A novel fuzzy logic-controlled Vienna rectifier to extract maximum power in the grid-connected wind energy system applications," in *Green Energy and Technology*, 2023, pp. 3–21, doi: 10.1007/978-981-16-8274-2_1.

[24] I. Ahmed *et al.*, "Recent advancement of AC–DC SEPIC converter: a state–of–the–art review on topologies, technical aspects and applications," *Results in Engineering*, vol. 27, 2025, doi: 10.1016/j.rineng.2025.106814.

[25] M. Atallah, M. A. Benmahdjoub, I. Salhi, A. Mezouar, Y. Saidi, and A. Gaillard, "Efficient nonlinear integral backstepping control for doubly fed induction generators-based wind farm under unbalanced electrical grid voltage," *International Journal of Electrical Power and Energy Systems*, vol. 172, 2025, doi: 10.1016/j.ijepes.2025.111141.

[26] M. Martínez-Rojas, C. Cano, J. Alcalá-Fdez, and J. M. Soto-Hidalgo, "Interpretable fuzzy control for energy management in smart buildings using JFML-IoT and IEEE Std 1855-2016," *Applied Sciences*, vol. 15, no. 15, 2025, doi: 10.3390/app15158208.

[27] M. S. Rahman and M. H. Ali, "Adaptive neuro fuzzy inference system (ANFIS)-based control for solving the misalignment problem in vehicle-to-vehicle dynamic wireless charging systems," *Electronics*, vol. 14, no. 3, 2025, doi: 10.3390/electronics14030507.

BIOGRAPHIES OF AUTHORS

Naveena Sandhadi is a research scholar in the Department of Electrical Engineering at the College of Engineering, Andhra University, Visakhapatnam, India. She has earned her M.Tech. from Gayatri Vidya Parishad College of Engineering with a specialization in power electronics and drives. Her research interests are electric vehicles. She can be contacted at email: sandhadinaveena211@gmail.com.

Dr. Srinu Naik Ramavathu is an associate professor in the Department of Electrical Engineering at the College of Engineering, Andhra University, Visakhapatnam, India. He earned his Ph.D. from the same university with a specialization in power systems, electrical earthing, and non-conventional energy systems. With over 25 years of academic experience, he has served in various roles, ranging from teaching assistant to assistant professor and associate professor. He has successfully guided doctoral research, published numerous research articles, book chapters, and books, and continues to contribute actively to advancements in power engineering and renewable energy. He can be contacted at email: drsrinunaikr@gmail.com.